Full Length Research Paper

The effectiveness of electrical resistivity imaging in sinkhole investigations

Nart COŞKUN

Department of Geophysics, Nevşehir University, 50300, Nevşehir, Turkey. E-mail: n_coskun@yahoo.com.tr.

Electrical resistivity methods are generally used to explore buried sinkholes and to predict dropout, sinkholes is analysed. A sinkhole of known geology is used to illustrate the limitation of vertical electrical sounding technique. Approximated geological sections of the sinkhole are modelled to investigate the effectiveness of the resistivity imaging which is considered to be two-dimensional exploration approach. The current study demonstrates that the resistivity imaging method is able to constrain the subsurface geological information for engineers, and to decide if soil improvement is needed for these regions of e.g. karstic terrain. If appropriate array distances, comparable to diameter and the depth of sinkhole are selected, the stratigraphy and the structure of the sinkholes can be mapped effectively, and to assess the potential for the future sinkhole development is monitored easily.

Key words: Resistivity imaging, sinkholes.

INTRODUCTION

Sinkholes are naturally occurring geological features that are commonly formed when rain falls dissolve limestone creating underground voids. Depending on the overlying layer (e.g. sandy or a loose material collapsing into these voids), a sinkhole can result (Figure 1). Sinkholes, subject of geosciences and geotechnical engineering are the characteristic features of the karstic terrains. Geomorphologists call these depression zones dolines. Slope failure, strain release and soil collapse may threaten life and livelihood when these occur in areas close to population, dam, sports arena and highway.

Filled sinks and channels are potential targets for mining geophysics. Ore bodies and mineralized zones are associated with filled sinks, which are locally considered as shale sinks. Prediction and mapping of the potential sinkholes is feasible, because of the developed physical property contrasts within the host rock. At this point of view, filled sinkholes and potential sinkholes have similar physical property contrasts with their environment to explore using geophysical methods. Therefore, prediction of the sinkholes is possible using geophysical methods.

Conventional methods for underground exploration on karsts are not adequate when the subsurface is complex.

Site conditions and target size are effective on the success of field survey. Even direct sampling alone may not be adequate to characterize some small targets, such as cavities, fractures and cracks. The geophysical methods are often used to investigate the subsurface and help reduce the exploration cost. However, care should be taken about these limitations due to site-specific conditions. The most commonly used geophysical methods are ground penetrating radar (GPR), self-potential (SP), electromagnetic (EM), electrical resistivity, time domain reflectometry (TDR), seismic methods (seismic tomography) and microgravity surveys.

GPR is a commonly used method for sinkhole investigations because of its ability to resolve details of shallow soil and rock conditions. This method is site specific and clay and/or high conductivity pore fluids limit the depth penetration. The combined effectiveness of GPR and standard penetration test (SPT) methods is investigated in residential sinkholes in West-Central Florida (Zisman et al., 2005). An 80% correlation between the two methods was found in 93 different sites and also, the limitations of the GPR method were discussed. For the same area, GPR and electrical resistivity methods were used to image the sinkholes of hydrogeological

Figure 1. Agricultural sinkholes from central Turkey.

significance. Three-dimensional (3D) GPR surveys hold promise for imaging such structures (Kruse et al., 2006). In another study by Hudyma et al. (2005), GPR, electrical resistivity and microgravity methods were used along with closely spaced boring to characterize a retention pond with previous sinkhole activity. They concluded that both traditional intrusive exploration techniques and geophysical surveys were required to characterize the subsurface.

The self-potential and electromagnetic (EM-34) methods are used to locate sinkholes in chalk substratum (Jardani et al., 2007). The two-dimensional (2D) electrical resistivity tomography (ERT) and TDR methods are used to characterize the hydrogeology and recharge mechanism in agricultural sinkholes (Schwartz and Schreiber, 2005). Ground subsidence problems are evaluated in urban areas. Integrated geophysical surveys (2D resistivity, controlled source magnetotelluric (CSMT), magnetic and cross-hole ERT and rock engineering investigation results were used for remediation programs (Kim et al., 2007). Multi-channel surface wave data (MASW), 2D electrical resistivity and SPT methods were used to investigate a catastrophic sinkhole in a residential area in Nixa Missouri (Robison and Alderson, 2008), where detailed information was obtained for the sinkhole and its vicinity. From the geophysical traverses, no evidence of threat was found for the neighbourhood. 2D electrical resistivity method was used by Van Schoor

(2002) to discriminate developing sinkholes and mature sinkholes comprising resistive air-filled (or water-filled) cavities.

Herein, we do not consider the classification of karsts ground conditions. Detailed information can be found elsewhere (Waltham and Fookes, 2005; Dobecki and Upchurch, 2006). Since filled sinkholes and potential sinkholes have similar electrical resistivity or conductivity contrast mapping and prediction of the potential sinkholes should be investigated in detail using resistivity imaging method. We aim to assess detailed information of buried sinkholes and predict dropout sinkholes for the benefit of civil engineering, mineral prospecting, agricultural and environmental purposes.

MATERIALS AND METHODS

In the electrical method, a current was introduced into the ground by two electrodes. The resulting potential differences were measured using two other electrodes. A geometric factor is needed to convert the readings obtained with the four-electrode into ground resistivity. From the potential measurements made at the surface, we gain information about the subsurface. Array configurations made of infinite number of four-probe (or more than four probes) are possible for a resistivity method. Wenner, Schlumberger and dipole-dipole and their orientations are commonly used in the field to acquire data. Figure 2 shows Wenner and Lee arrays along with their specific electrode positions and spacing.

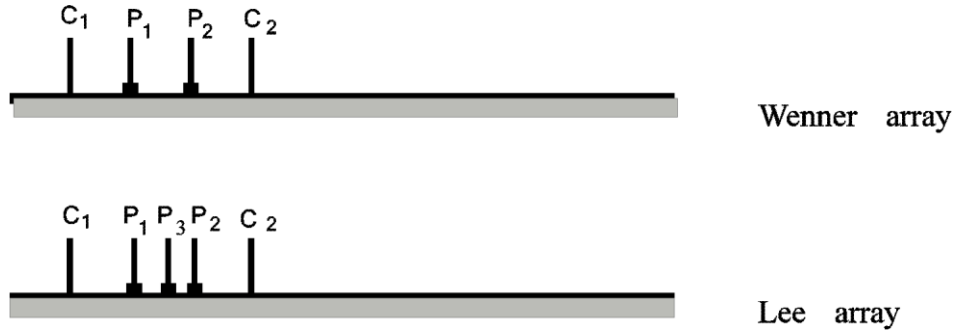The Wenner configuration has probes spaced at equal intervals.

Figure 2. Wenner and Lee arrays.

The outer probes apply current and the inner pair measure potential difference. This array has good vertical resolution. The Lee array resembles the Wenner array, but has an additional central electrode. Two measurements are made using the three potential electrodes; the mean value of the two measurements is used in this work.

For each set of probe positions, the apparent resistivity is usually calculated by Equation 1.

$$\rho = G \frac{\Delta V}{I} \tag{1}$$

where ΔV = potential difference measured between P_1 and P_2 electrodes; I = current between C_1 and C_2 electrodes; and

$$G = \frac{2\pi}{\dfrac{1}{r_1} - \dfrac{1}{r_2} - \dfrac{1}{r_3} + \dfrac{1}{r_4}}$$

where r_1, r_2, r_3 and r_4 define distances C_1P_1, C_2P_1, C_1P_2 and C_2P_2, respectively. For the Wenner array, a = inner electrode spacing so that Equation 1 becomes:

$$\rho_w = 2\pi a \frac{\Delta V}{I} \tag{2}$$

For a homogeneous conducting medium, the calculated value of resistivity is independent of probe positions and spacing, but in reality, this is not the case and the measurements will vary with the relative positions of the electrodes. Under these circumstances, the geometric constant becomes a position-dependent approximation.

$$\rho_{aw} = 2\pi a \frac{\Delta V}{I} \tag{3}$$

The calculated value of resistivity is referred to as apparent resistivity and shown by ρ_a where the SI unit of ρ_a is ohm-meter.

The subsurface may be explored by three main procedures called electrical horizontal profiling (or trenching), vertical electrical sounding (VES) and combined sounding-profiling which is adopted for automatic data acquisition systems. Profiling is usually done with fixed electrode spacing. Near-surface resistivity variations can be detected by using smaller electrode spacing. Buried features can be located and identified due to their contrast in physical properties

against the host rock and soil. In the VES technique, the distances between some or all the electrodes are systematically increased to investigate the layered media. The used field data in this study is acquired in this fashion using Lee array from Cherokee County, Kansas (Van Nostrand and Cook, 1966). In the combined sounding-profiling technique, measurements are made along a profile with selected electrode spacing with a multi-electrode system. Electrode spacing repeatedly increased for each step. Apparent resistivity pseudo-sections are produced using this technique.

VES approach

Figure 3a is an observed VES data obtained over the centre of a filled sink consisting of left and right Lee configurations at both sides (Van Nostrand and Cook, 1966, page 229). Figure 3a shows two curves corresponding to right-side Lee array (ρ_1 EAST) and left-side Lee array (ρ_2 WEST). The centre of both arrays is located at the middle of sink where the middle drill-hole is placed.

Figure 3b shows geological cross section defined by data obtained from six drill-holes. The region corresponds to the vicinity of known shale sink in the Tri-State lead-zinc mining district, Cherokee County, Kansas. An alluvium bowl tops the hemispherical filled sink. Sandstone, clay and shale layers lie beneath the alluvium. Depths to the interfaces obtained from the drill-hole in the middle of the sink are as follows:

1. Alluvium: sandstone and clay interface (8.5 m)
2. Sandstone and clay: shale interface (16.0 m)
3. Shale: limestone interface (28.0 m)

The right-side Lee array (ρ_1 EAST) and left-side Lee array (ρ_2 WEST) curves are digitized and converted into a single Wenner array (Figure 4).

VES interpretation

The VES Wenner data obtained from the Lee array were inverted using an inversion program based on the following equation (Parasnis, 1986):

$$S = \sum_{i=1}^{N} \left[y_i - \rho_a \left(x_i, P_j \right) \right]^2 \tag{4}$$

where ρ_a (x_i, P_j) is the apparent resistivity for x_i on the model represented by the set P_j. $P_j (j=1,2,...,m)$ is the starting model with n
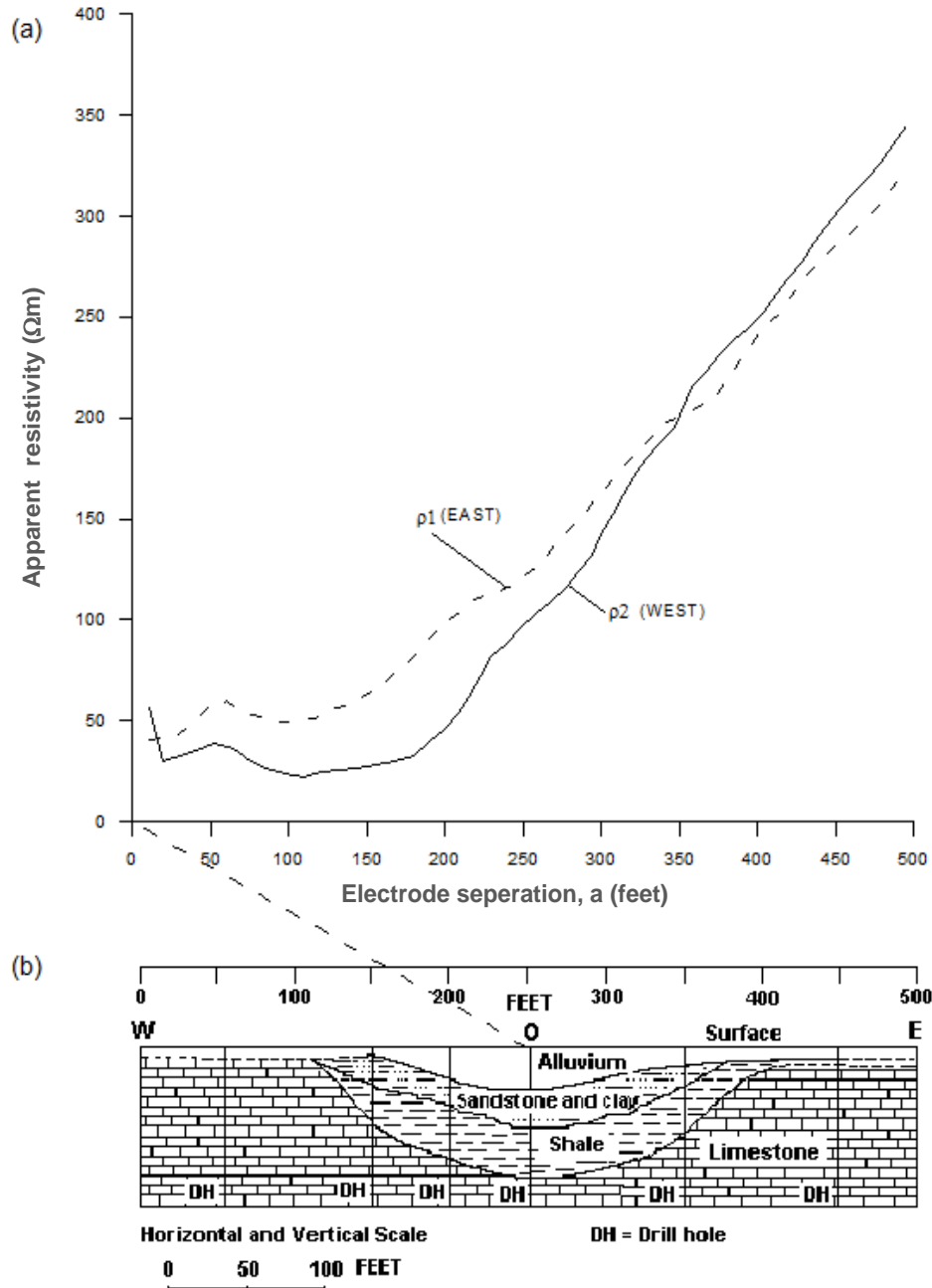
Figure 3. (a) Observed VES data at station approximately over centre of hemispheroidal filled sink, Tri-State lead-zinc mining district, Cherokee County, Kan., Lee array (Van Nostrand and Cook, 1966, page 229) and (b) geological cross section.

resistivities and (n-1) layer thicknesses, the *nth* layer being the substratum, therefore, $m=2n-1$. Measured value of ρ_a is y_i for the N separations $x_i(i=1,2,....,N)$ between the current electrodes. An iterative procedure is used to produce an optimum model. Optimization method minimizes the sum of squares of difference between the observed and calculated ρ_a values.

We know that when the layered medium is not parallel (dipping) and has lateral discontinuities, the interpreted VES curve may produce more layers than that of the actual subsurface. The peaks and lows on the apparent resistivity curves may be misleading the interpreter. HKHA type ($\rho_1 > \rho_2 < \rho_3 > \rho_4 < \rho_5$) 5 layer case will result

when this Wenner sounding curve is evaluated. Interpreted results (Table 1) obtained using an algorithm based on Equation 4 for the Wenner array VES curve are given in Figure 4.

The filled sink has asymmetrical geometry, and there exists some contrast on the contact between materials in the sink and the surrounding. When interpreted in one-dimensional (1D), apparent resistivity measurements model this contact as pronounced discontinuity. Many factors affect the result obtained from the interpretation of the measured data. These mainly depend on the level of experience with the employed method and on the sound knowledge of underground geology that if dipping contacts, vertical

Table 1. Interpreted result of Wenner VES curve.

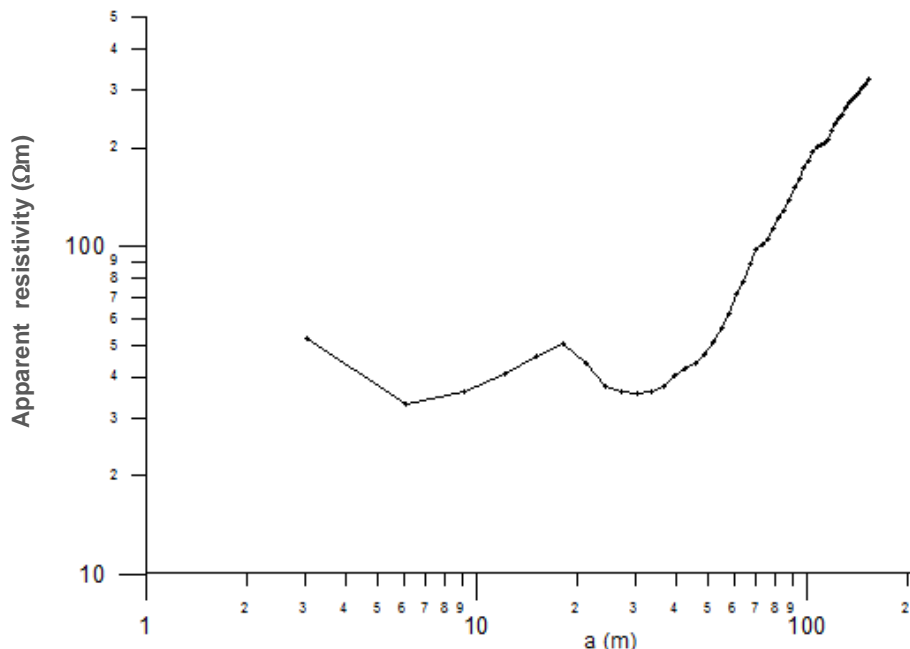| Resistivity (Ωm)	h-layer thickness (m)	d-layer depth (m)
$\rho_1 = 61.9$	$h_1 = 2.0$	$d_1 = 2.0$
$\rho_2 = 23.8$	$h_2 = 7.32$	$d_2 = 9.32$
$\rho_3 = 2233$	$h_3 = 19.3$	$d_3 = 28.32$
$\rho_4 = 28.8$	$h_4 = 12.4$	$d_4 = 40.72$
$\rho_5 = \infty$	$h_5 = \infty$	$d_5 = \infty$

Figure 4. Wenner array VES curve of Figure 3a.

contacts and metallic conductors exist within the medium. The VES curve may display distinct features that are helpful hints in the interpretation of local geology. The interpreter should know how and to what extend 1D approximations represent the earth's true subsurface. A detailed knowledge of the geology should not be expected from a few tens of 1D measurement if especially the subsurface is complex.

Combined sounding-profiling approach

In the combined sounding-profiling data acquisition technique, the electrode spacing is repeatedly increased at each step. Figure 5 shows the first step. When the electrode spacing is increased, the plotting values get deeper from which a depth dependent pseudo-section is built.

Modelling example

Figure 6 shows approximated model of geologic section (Figure 3b). The section used to produce two different pseudo-section for two minimum Wenner electrode separation (a = 7.62 and a = 15.24 m). Six different steps were used for Wenner array and combined sounding-profiling responses were calculated as pseudo-section

using forward modelling technique.

Forward modelling method

The forward modelling of the theoretical models used in this work have been performed using the finite element method (FEM). Since the method has been extensively described in many works (Coggon, 1971; Rijo, 1977; Sasaki, 1982; Wannamaker, 1992; Loke and Barker, 1996a), a brief description of the method is presented here.

The FEM solves the Helmholtz equation by discretizing the earth into homogeneous triangular regions called elements. The potential within each element is approximated by a simple interpolatory function, that is, the basis function, and is related to the potential at the nodes of each triangle. To minimize the error between the approximated and real potential, the Galerkin minimization criterion is applied. The individual element equations can be assembled into one global system as the following.

$$Lf = s, \qquad (5)$$

where f is the unknown transformed nodal potential vector, s is a vector describing the sources and L is a matrix that is related to the nodal coordinates. After applying the boundary conditions, the
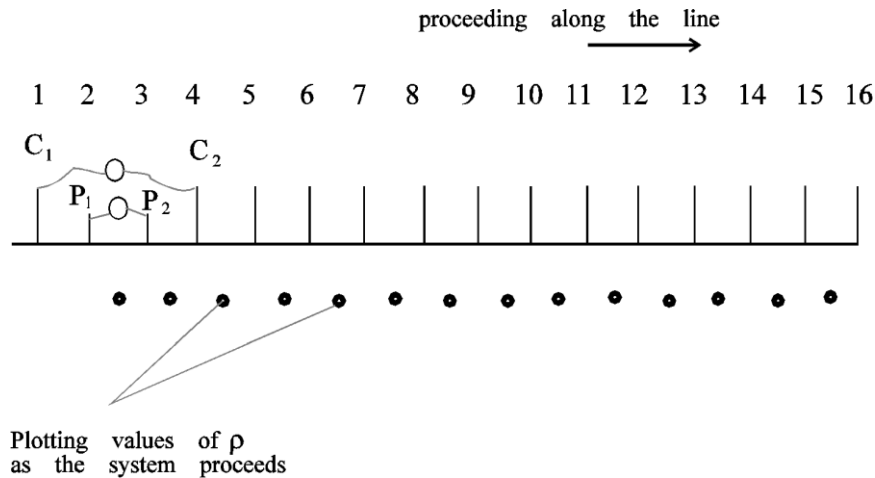
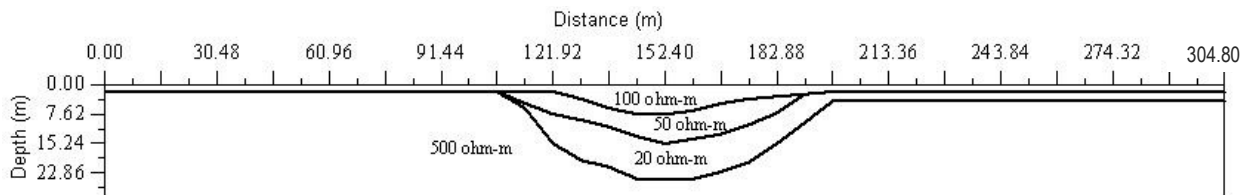**Figure 5.** The procedure for the Wenner array.

Figure 6. Approximated model of geological section given in Figure 3b.

system of Equation 5 is being solved and the transformed nodal potential is obtained. After solving Equation 5 for several wave-numbers, the total potential is recovered by applying the inverse Fourier transform. Since the nodal potential is known, point-to-point potential differences are obtained, and then apparent resistivities for given electrode arrays are calculated by Equation 6 that is similar to Equation 1.

$$\rho_a = G\,\Delta V/I \qquad\qquad (6)$$

where I is current source, ΔV is the potential difference and G is the geometric factor which is dependent on the type of electrode array and spacing used.

The apparent resistivity pseudo-sections are calculated from the approximated model of geologic section (Figure 6) using finite-difference method (FDM) briefly described earlier. Figures 7 and 8 show calculated pseudo-sections for a=7.62 and 15.24 m, respectively. The data given in Figures 7 and 8 are assumed to represent the field data obtained over a buried sinkhole. The data obtained from the models were inverted using the inversion program.

Resistivity imaging

Inversion process is used to determine the structure of the subsurface by analysing the field measurements of electrical resistivity method. In this work, field data is created for combined sounding-profiling approach from the 2D model using forward modelling technique. The aim is to obtain an accurate earth model which represents the actual subsurface (Figure 6 in this case). The modelling schema consists of an inversion process based on an iterative method that minimizes the difference between measured

pseudo-section and a pseudo-section calculated from the model. The model is modified until acceptable agreement is covered. This is expressed as measured by the root mean squared (RMS), after five iterations agreement reached 3% RMS error. Care should be taken accepting the theoretical model presenting correct geological section.

The approach used in 2D model case is similar to 1D case, given in VES interpretation section.

Figure 9a shows the inverse model section for minimum electrode distances of 7.62 m, while Figure 9b corresponds to the case of 15.24 m. The diameter and the depth of the sinkhole are about 93 and 26 m, respectively. Cover layer of alluvium varies from 3 to 7 m. Figure 6 is re-drawn in Figure 9c to visually inspect the similarities between the inverse model resistivity sections and the geological cross section. It can be seen from Figure 9a that the stratigraphy of the sinkhole is effectively mapped for minimum electrode separation of 7.62 m. The diameter obtained more for the minimum electrode separation of 15.24 m and less information yielded for layers. When compared with the previous 1D interpretation (VES interpretation), the 2D inversion method is more reliable to highlight the details of the complex subsurface.

RESULTS AND DISCUSSION

In the 1D case, it is assumed that the ground corresponds to a horizontally layered model. In practice, this requirement is fulfilled if the dip of the layers is less than 10^0. The 1D case is very often assumed for vertical electrical soundings. In any case, the possibility of 2D or 3D effects must be taken into consideration when the
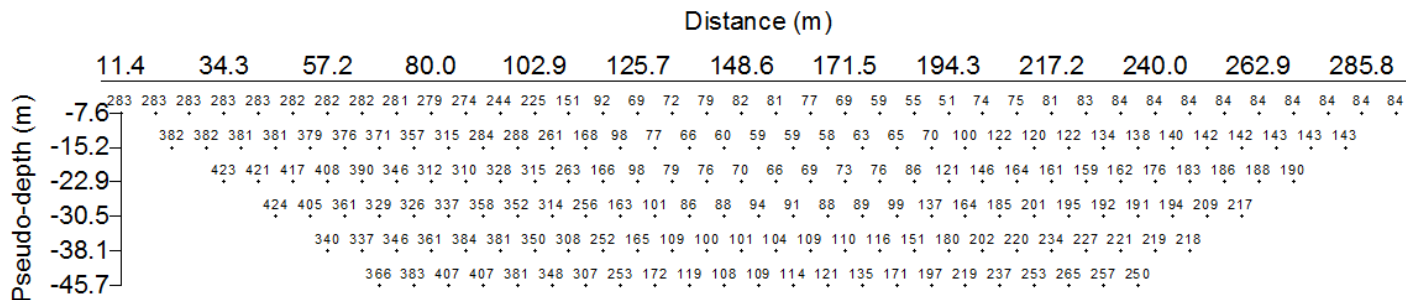
Figure 7. Theoretically calculated apparent resistivity pseudo-section of Figure 6. Minimum electrode distance is 7.62 m.
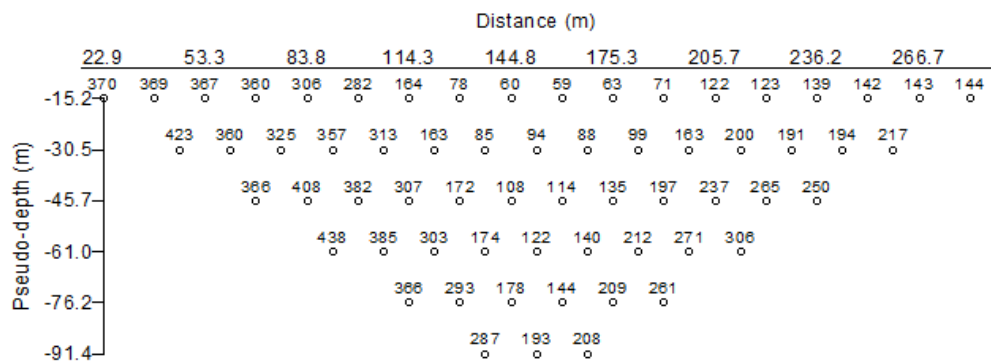

Figure 8. Theoretically calculated apparent resistivity pseudo-section of Figure 6. Minimum electrode distance is 15.24 m.
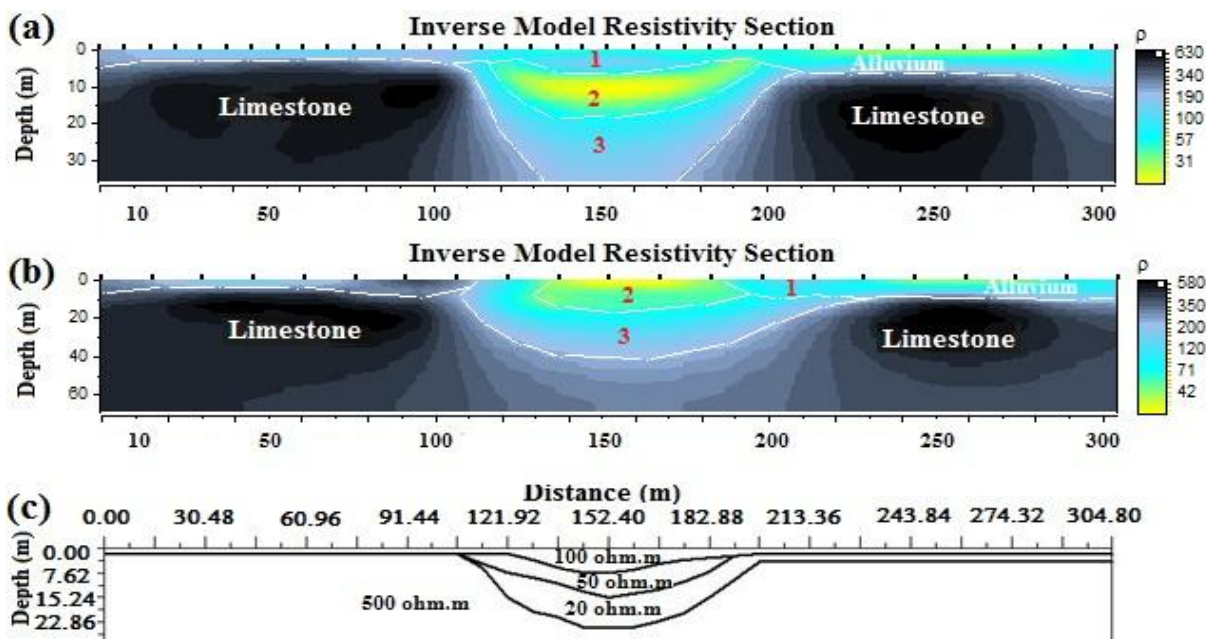

Figure 9. (a) Wenner 7.62 m inverse model section; (b) Wenner 15.24 m inverse model section; (c) Approximated model of geological section given in Figure 3b. Layering in sinkhole denoted as 1, 2 and 3 on both inverse model sections.

sounding survey is planned.

The resistivity imaging results imply that the selection of the appropriate array distance and sound geological knowledge is important for the effective application of the electrical resistivity method. Therefore, after reconnaissance electrical resistivity surveys (taking the array distances wide), conducted detailed surveys needed to assess detailed information from the filled and potential sinkholes.

Conclusion

If appropriate array distances are selected, the stratigraphy and the structure of the sinkholes can be mapped effectively and assessment of the potential sinkhole is feasible, because of the electrical conductivity contrast developed between country rock and dissolved features within. The resistivity imaging method can also provide important information on the grout volumes against which stabilization of overburden may be needed. By highlighting the physical properties of underground geology, the resistivity imaging method can help avoid litigations and disputes between property owners and insurance or legal experts.

REFERENCES

Coggon JH (1971). Electromagnetic and electrical modelling by the finite element method, Geophysics, 36: 132-155.
Dobecki TL, Upchurch SB (2006). Geophysical applications to detect sinkholes and ground subsidence. The Society of Exploration Geophysicists, The Leading Edge, 25 (3): 336-341.
Hudyma N, Ruelke TJ, Samakur C (2005). Characterization of a Sinkhole Prone Retention Pond Using Multiple Geophysical Surveys and Closely Spaced Borings. ASCE Conf. Proc. doi:10.1061/40796(177)59.
Jardani A, Revil A, Santos F, Fauchard C, Dupont JP (2007). Detection of preferential infiltration pathways in sinkholes using joint inversion of self-potential and EM-34 conductivity data, Geophys. Prospect., 55 (5): 749–760.
Kim J-H Yi M-J, Hwang S-H, Song Y, Cho S-J, Synn J-H (2007). Integrated geophysical surveys for the safety evaluation of a ground subsidence zone in a small city. J. Geophys. Eng., 4 (3): 332–347.
Kruse S, Grasmueck M, Weiss M, Viggiano D (2006). Sinkhole Structure Imaging in Covered Karst Terrain. Geophys. Res. Lett., 33: L16405, Doi: 10.1029/2006gl026975.
Loke MH, Barker RD (1996a). Rapid least-squares inversion of apparent resistivity pseudosections using a quasi-Newton method, Geophys. Prospect., 44: 131-152.
Parasnis DS (1986). Principles of Applied Geophysics. Fourth Edition, Chapman and Hall, New York. p. 402.
Rijo L (1977). Modelling of electric and electromagnetic data. University of Utah, Salt Lake City, Ph.D. Thesis, p. 242 (unpublished).
Robison JL, Anderson NL (2008). Geophysical Investigation of the Delaware Avenue Sinkhole Nixa, Missouri. ASCE Conf. Proc. doi:10.1061/41003(327)7.
Sasaki Y (1982). Automatic interpretation of induced polarization data over two-dimensional structures. Memoirs of the Faculty of Engineering, Kyushu University, 42: 59-74.
Schwartz BF, MSchreiber E (2005). New applications of Differential Electrical Resistivity Tomography and Time Domain Reflectometry to Modelling Infiltration and Soil Moisture in Agricultural Sinkholes, ASCE Conf. Proc. doi:10.1061/40796 (177)58.
Waltham AC, Fookes PG (2005). Engineering classification of karst ground conditions, Speleogenesis and Evolution of Karst Aquifers, The Virtual Scientific J. ISSN 1814-294X, www.speleogenesis.info Re-published from, Quarterly. J. Eng. Geol. Hydrogeol., 2003, 36: 101-118.
Wannamaker PE (1992). IP2DI-v1.00: Finite element program for dipole-dipole resistivity/IP forward and parameterized inversion of two-dimensional earth resistivity structure. University of Utah Research Institute, Report No-.ESL-92002-TR, p. 62 (unpublished).
Van Nostrand RG, Cook KL (1966). Interpretation of resistivity data, U. S. Geological Survey Professional, p. 499. at http://books.google.com/
Van Schoor M (2002). Detection of sinkholes using 2D electrical resistivity imaging, J. Appl. Geophys., 50 (4): 393–399.
Zisman ED, Wightman MJ, Taylor C (2005). The Effectiveness of GPR in Sinkhole Investigations, ASCE Conf. Proc. doi:10.1061/40796 (177)65.